

## STATE-OF-THE-ART REVIEW OF PRECAST BRIDGE COLUMNS WITH RE-CENTERING SEISMIC RESPONSE

**Joshua T. Hewes**, Ph.D., PE, Dept. of Civil Eng., Construction Management, and Environmental Eng., Northern Arizona University, Flagstaff, Arizona

**Rebecca Braley**, Dept. of Civil Eng., Construction Management, and Environmental Eng., Northern Arizona University, Flagstaff, Arizona

### ABSTRACT

*Significant research on the behavior of self-centering concrete bridge column has been conducted in the last decade. Research has been driven by a desire for improved earthquake performance and by the national push towards accelerated bridge construction, spearheaded by the U.S. Federal Highway Administration (FHWA). It has been shown that reduced damage can be achieved under high seismic loading. However, no official design standards have been created. This paper presents a detailed review of past research, and an analysis of future research needed to advance the state-of-the-art to a point where bridge owners can confidently embrace this promising technology.*

*Many issues require additional research such as: What level of initial tendon prestress is “ideal”? What are the confinement requirements and details near regions of gap opening? How much supplemental damping should be included? What are the performance limit states for the system? Should a force-based design or direct displacement-based design methodology be used? If force-based design, what strength reduction factors are appropriate? If direct displacement-based design, what are the appropriate equivalent damping versus displacement ductility relationships? What shear reinforcement is required? An in-depth discussion of the above issues and implications of possible solutions is provided.*

**Keywords:** Unbonded, Seismic, Precast, Bridge, Re-center

## **INTRODUCTION**

In the last two decades since 1990, there has been significant research focused on the development of technologies to improve the seismic performance of concrete buildings and bridges. One concept, first developed for the precast concrete building industry, focused on reducing material damage at critical sections within main structural elements and on enhancing overall post-earthquake serviceability by minimizing residual deformations in the structure. These aims were achieved via the use of unbonded post-tensioned longitudinal reinforcement, and the technology was developed and validated in the comprehensive research program “PREcast Seismic Structural Systems” or “PRESSS” Program which culminated in the structural testing of a 60% scale five-story building.

Based on the success of the PRESSS Program, researchers in the late 1990’s applied the unbonded post-tensioning reinforcement technology to precast concrete bridge columns and demonstrated that reduced overall earthquake damage could be achieved as compared to traditional reinforced concrete (RC) columns. In the column with unbonded post-tensioned tendons, the lengthening or stretching of the steel associated with column curvature is not proportional to curvature at a given section but rather is uniform along the column height. Thus, the very large reinforcement normal strains that are concentrated in the plastic hinge regions of traditional RC columns are avoided, and the unbonded post-tensioning force re-centers the system once lateral seismic forces have subsided. The residual drift of a conventional RC column after a moderate earthquake will be on the order of 1% to 2% while that for a column with unbonded tendons is expected to be on the order of 0.1% to 1%. Moreover, the significant material damage often observed in the plastic hinge zones of conventional columns can be avoided in the unbonded tendon column with proper detailing.

In the sections that follow, an in-depth review of research on bridge columns with unbonded post-tensioned main longitudinal reinforcement is provided. Following the review, a discussion of the critical aspects of unbonded column design which have yet to be fully studied or that lack specific design guidelines are described.

## **REVIEW OF PAST RESEARCH**

This section contains descriptions of major research efforts that have investigated the behavior, analysis, and design of bridge columns incorporating unbonded post-tensioning for the purpose of producing a re-centering characteristic under seismic loading. The review of past research is organized by institution where the majority of the work took place, rather than by specific individual name. Publications that describe small investigations into this relatively new column system are not reviewed in this paper.

## **UNIVERSITY OF CALIFORNIA SAN DIEGO**

This experimental and analytical research program was one of the first to investigate the seismic behavior of unbonded post-tensioned columns, both experimentally with large-scale testing and with analytical studies. The work was reported on in publications by Hewes and

Priestley<sup>1</sup> and Hewes<sup>2, 3</sup>, and the focus of the research was on the design, construction, and testing of four segmental precast concrete columns under simulated lateral seismic loading and the development of an analytical model to predict their lateral force – displacement response.

All of the test columns included a single unbonded post-tensioned tendon concentric with the circular column cross-section, and steel jacket confinement at the column base, with no mild steel rebar continuous across segment joints. Precast segments above the base segment (directly above footing level) utilized standard transverse mild steel spiral reinforcement. Of the four test columns, two had an aspect ratio of three and two had an aspect ratio of six, where the aspect ratio is defined as the height from column base to point of contraflexure divided by the column diameter ( $L/D$ ). Concrete compression strengths ranged from about 40 MPa to 58 MPa on test day, and for each aspect ratio, one test column had a steel jacket with transverse volumetric confinement ratio of 2% and the other 4%. One of the key parameters that influences unbonded column seismic response is the level of initial concrete axial stress, which is due to column axial gravity loads and the initial post-tensioning force in the tendons. The dimensionless “axial force ratio”, or “AFR”, is defined as:

$$AFR = \frac{P + T}{f'_c A_c} \quad (1)$$

where  $P$  is the gravity load,  $T$  is the tendon post-tensioning force,  $f'_c$  is the concrete compression strength, and  $A_c$  is the column concrete cross sectional area. The range of AFR tested was 0.19 to 0.28. One additional key aspect of the research work is that after each column was tested, it was repaired via epoxy injection any residual cracks and post-tensioned to a higher initial tendon force, and tested a second time.

Key findings of the research include validation of the technology as a viable alternative to conventionally reinforced concrete columns because of its stable, ductile lateral force – displacement response, and the reduced damage as compared to traditional RC columns. Residual lateral deformations of the unbonded columns were minimal, as seen in Figure 1(a) below which shows the force – displacement response for a low aspect ratio column with 4% lateral base confinement (volumetric ratio of transverse reinforcement with respect to the core concrete). The figure also reveals the one significant drawback to using exclusively unbonded longitudinal reinforcement: there is very little energy dissipated by the system as evidenced by the pinched hysteretic response and thin hysteresis loops. Also evident in Figure 1(a) is the ability of the simple analytical model developed in the research to predict the lateral force – displacement response as a function of column parameters including aspect ratio, concrete compression strength, tendon unbonded length, cross sectional area, and initial stress, location of the tendon within the section depth, transverse confinement at the base, and axial gravity load.

The model described by Hewes and Priestley assumes lateral deformation of the unbonded column is due primarily to rocking about its base compression edge and uses overall member compatibility and moment – curvature analysis of the base column section to determine

member strength versus deformation. Member deformation compatibility is used because traditional strain compatibility between concrete and steel strains at a given section is not valid as a result of the unbounded nature of the prestressing tendon. Tendon incremental strains are calculated by Equation 3, where the base flexural crack opening angle is assumed equal to the overall column drift angle, as shown in Figure 4. An analogy is made between the unbounded column and traditional monolithic RC construction, and a plastic hinge length,  $L_p = D/2$  is assumed. Thus, the base column section curvature,  $\phi$ , can be related to overall column drift,  $\theta$ , and a conventional section moment curvature analysis is performed to determine moment resistance and the particular drift level.

Figure 1 (b) below illustrates the dramatic influence of the AFR parameter on column behavior as predicted using the simple analytical model ( $F_{si}$  in the figure is initial prestress force). Low initial AFRs lead to very ductile seismic response with relatively large post-yield (or second-slope) stiffness, while higher initial AFRs on the other hand increase column strength at the expense of reduced ductility – smaller post-yield stiffness and ultimate displacement capacity. The influence of AFR on second slope stiffness is explained as follows. The AFR determines the total vertical axial force (gravity load plus post-tensioning force) acting at the column base and hence influences the position of neutral axis depth,  $c$ . For low AFRs and their corresponding smaller neutral axis depths, the gap opening at the column base is larger and hence leads to larger increases in tendon force, which in turn leads to larger resisting moments. For high AFRs, the neutral axis depth is larger for the same drift level based on satisfying vertical force equilibrium, and hence there is less gap opening at the base and tendon force increase. Thus, there is less increase in resisting moment. The softening behavior with negative second-slope stiffness for columns with high AFR is a result of the higher concrete compression strains, which are necessary to satisfy vertical equilibrium and member deformation compatibility, which result in movement of the concrete compression centroid towards the section centroid rather towards the extreme compression fiber of the critical section.

The analytical model used by Hewes and Priestley has also been developed by others for use on columns incorporating both unbonded post-tensioning and mild steel for enhanced energy dissipation, and it has been shown repeatedly to provide excellent prediction of column response when compared to experimental test results. Hence, an engineer can easily evaluate column lateral seismic response and tailor the initial post-tensioning force to achieve the desired behavior. In order to balance the competing needs of system ductility and economical use of the column section (i.e. maximize strength for a given column size), Hewes and Priestley's research recommended an initial AFR of approximately 0.20 and an AFR of about 0.30 at maximum lateral displacement response

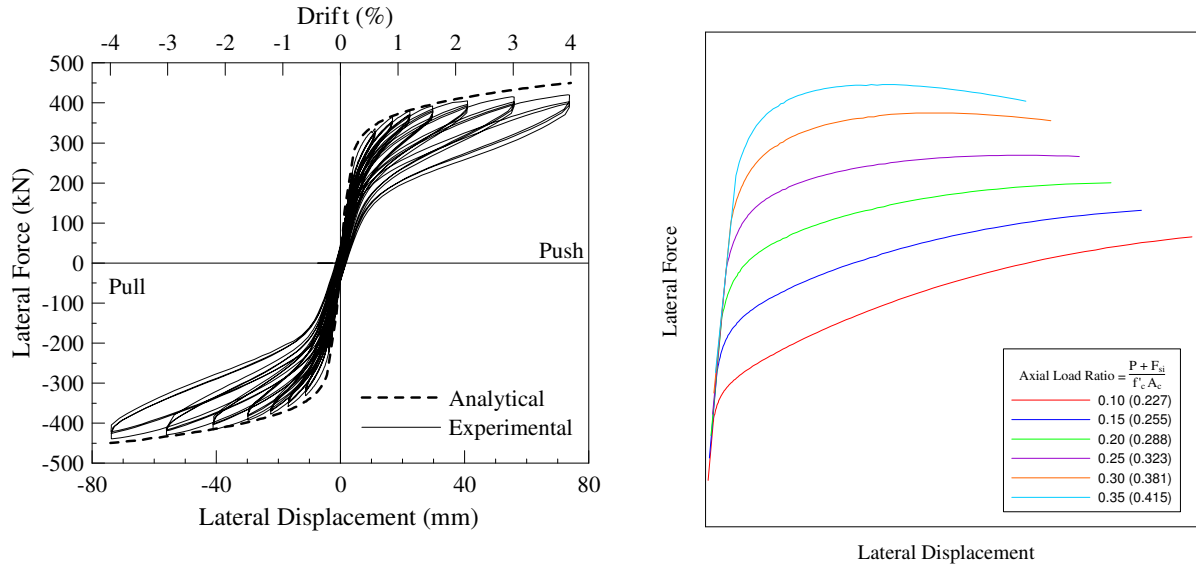


**Fig. 1 (a) Force – displacement response of unbonded PT column (b) Influence of AFR on unbonded PT column lateral force displacement response (from Hewes and Priestley<sup>1</sup>)**

## UNIVERSITY OF CANTERBURY

Researchers at the University of Canterbury in New Zealand investigated the performance of columns with unbonded post-tensioning and “hybrid” bridge piers via experimental and analytical studies (Marriott, Boys, and Pampanin<sup>4</sup>, Palermo, Pampanin, and Marriott<sup>5</sup>, and Marriott, Pampanin, and Palermo<sup>6</sup>). The hybrid bridge columns they investigated included both longitudinal unbonded post-tensioning and internal and external yielding mild steel reinforcement which is unbonded over a small length near the critical section and that serves to increase system energy dissipation. Experimental testing of 1/3-scale bridge columns was carried out on cantilevered columns subjected to quasi-static simulated lateral seismic loading, and the performance of unbonded post-tensioned and hybrid specimens was compared to that of a traditional cast-in-place monolithic reinforced concrete benchmark test specimen. The work also includes implementation of simple analytical models to predict the lateral force – displacement column response.

The primary parameters investigated in the research work included the ratio of re-centering moment to dissipative moment (moment resistance associated energy dissipation mechanisms), which was defined as:

$$\lambda = \frac{M_{PT} + M_N}{M_S} \quad (2)$$

where  $M_{PT}$  represents the moment contribution of unbonded tendons,  $M_N$  is the moment contribution of gravity load, and  $M_S$  is the contribution of yielding mild steel rebar to flexural resistance at the design displacement. The variable  $\lambda$  was identified as the critical design parameter because it serves to indicate the relative tendency of the hybrid column to re-center

upon unloading: for  $\lambda$  less than unity, the re-centering moments are less than the moment required to yield the mild steel back in the unloading direction and the self-centering aspect will not be attained. For  $\lambda$  greater than unity, the moments acting to re-center the column during unloading are greater than the moment required to yield the energy dissipation reinforcement and the self-centering characteristic will, ideally, be achieved. In addition to  $\lambda$ , the amount of yielding energy dissipation rebar was varied, with values of longitudinal reinforcement ratio ranging from 0.26% to 1%. Test columns were 350 cm square sections with concrete compression strengths ranging from 54 MPa to 65 MPa, and the unbonded tendons consisted of either two seven-wire strands or four seven-wire strands located along the principal axes of the section 5.8 cm from the section centroid.

Results of the research program highlighted the superior performance of the hybrid column compared to conventional RC column designs. Similar to the work by Hewes and Priestley, the lateral force – displacement response of columns with only unbonded post-tensioning was characterized by a flag-shaped behavior with the characteristic pinching of the hysteresis loops at the origin. It is noted that this column arrangement without the supplemental damping provided by yielding mild steel is not ideal since increased lateral seismic displacement demands are expected due to the low energy absorption of the system. For hybrid columns, damage was limited primarily to flexural cracks which closed completely after testing, and yielding or rupture of the mild steel energy dissipation bars. The observed influence of the re-centering ratio  $\lambda$  on hysteretic response confirmed that for lower values of  $\lambda$  “fatter” hysteresis loops and less re-centering occur, while higher values of  $\lambda$  produce a more flag-shaped response with increased re-centering characteristics. Values of  $\lambda$  reported in Palermo et al.<sup>5</sup> included 1.4, 2.34, and 5.34, with corresponding residual drifts of approximately 0.8%, 0.25%, and 0% respectively after achieving peak lateral drifts of 3.5%.

A comparison of predicted or analytical column response quantities to those measured during testing was conducted, and included comparisons of column drift, neutral axis depth, tendon force, and moment capacity at the yield, damage, and ultimate limit states. For all columns tested, very good agreement between the analytical and experimental values was observed. It is noted that the analytical predicted values of the above were determined using the “monolithic beam analogy” (MBA) model developed by Pampanin, Priestley, and Sritharan<sup>7</sup> originally for jointed ductile beam-column connections in precast concrete hybrid building systems. This model is very similar to that proposed for columns with only unbonded post-tensioning by Hewes and Priestley, except that it includes the effects of mild steel yielding rebar and utilizes a different expression for plastic hinge length,  $L_p$ .

A final important result of the work at Univ. of Canterbury is the ability of simple lumped-plasticity rotational spring models to predict the cyclic hysteretic response of the hybrid column system. The modeling approach proposed by the researchers is to use two rotational springs in parallel, with one spring representing the yielding dissipaters and the other representing the re-centering moment contributions of the post-tensioning and axial load, as depicted in Figure 2 (a). The moment – rotation behavior for each spring is determined using the simple MBA analytical model, and the ability of this modeling approach to capture overall hysteretic response is significant as it allows for the development of equivalent

viscous damping versus displacement ductility relationships as shown in Figure 2 (b) below. Shown in the figure is the calculated damping from experimental tests (grey line with dots) and that predicted using the two-spring lumped plasticity model (red dashed line with dots). By comparing the two, it is clear that the hybrid column damping can be very accurately modeled using the two-spring lumped plasticity approach. This is a critical since such relationships are required in the design of hybrid columns by the direct displacement-based design procedure which is discussed later.

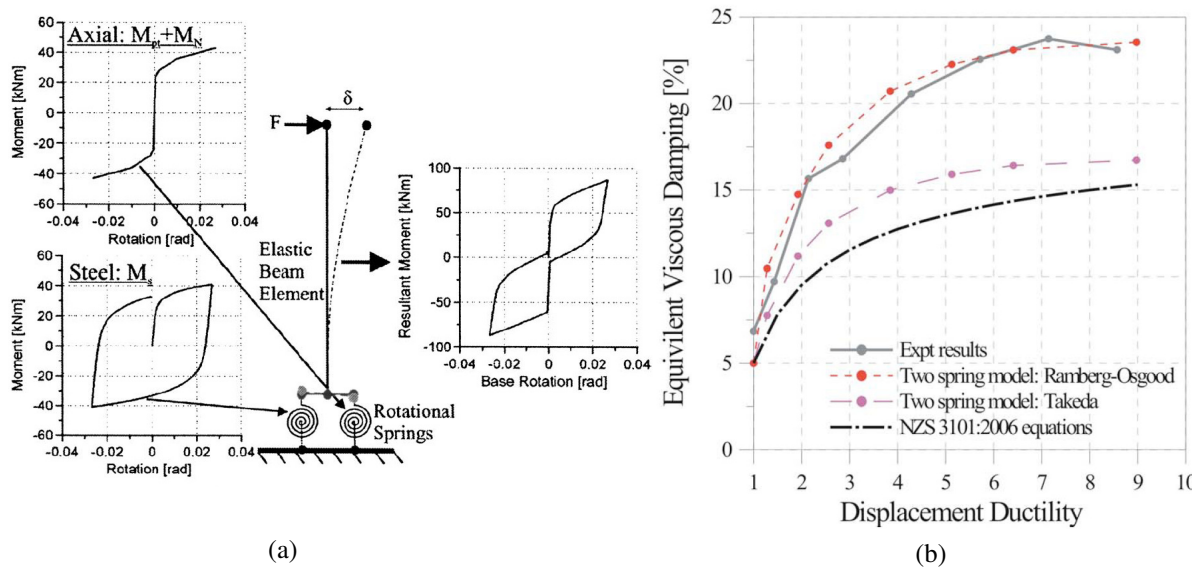


**Fig. 2 (a) Lumped plasticity model for hybrid columns, (b) Damping vs. ductility relationship (from Palermo et al.)**

#### NATIONAL CHIAO TUNG UNIVERISTY, TAIWAN

Studies by Chou and Chen<sup>8</sup> and Chou and Hsu<sup>9</sup> investigated the performance of two precast concrete-filled steel tube (CFT) bridge columns with unbonded post-tensioning reinforcement under simulated lateral seismic loading. The research work also refined the analytical model proposed by Hewes and Priestley via calibration against the experimental test data and by incorporation of a distributed plasticity model with two “plastic hinges” – one at the base of the first segment and one at the interface between the first and second segments. It is noted that plastic hinges as observed in conventional RC columns do not occur in the unbonded tendon column, but the analogy is made between traditional plastic hinges and the concentrated rotation that occurs at sections with significant gap opening in the re-centering column. The columns tested by Chou and Chen were at one-sixth scale and were circular in cross-section with a 500 mm outer diameter. Each column was composed of four precast segments, with the lowest or base segment encased in an A36 steel shell with 5 mm wall thickness, and other segments encased in 3 mm thick steel shells. Both test columns contained a single post-tensioned tendon located at the center of the section, and the segments did not contain any other longitudinal reinforcement. The initial AFR at the start of testing was approximately 0.25. Finally, one test column also included external energy

dissipation devices comprised of A36 plate steel anchored between the foundation and the base of the first segment.

Similar to findings reported by others as described above, both test columns exhibited stable, ductile flexural response up to the maximum imposed drift of 6%. Flag-shaped hysteretic behavior with pinching at the origin was observed in the lateral force – displacement response of both specimens, although the column with external yielding mild steel dissipaters showed slightly more energy absorption and residual displacement. Rotations at locations between the base of the first segment and footing level, and between the top of the first segment and bottom of the second segment were measured experimentally. Upon examination of the components of lateral displacement, it was found that column lateral deformation beyond early (elastic) stages of loading is due to both a rigid rotation of the column about its base (footing level) and to a smaller extent, about the top of the first segment. Based on these findings, the researchers proposed a two-plastic hinge model where inelastic rotations are concentrated at the column base and between the first and second segment.

In order to visually compare the various components of lateral displacement, the researchers plotted the ratio of predicted lateral displacement to the actual lateral displacement imposed during testing, as is shown in Figure 3 below. Figure 3 (a) shows the ratio of predicted lateral displacement to measured when a one plastic hinge (rotation about column base only) model is adopted, while Figure 3 (b) shows the displacement ratios when a two plastic hinge model is used. For each drift level, the first vertical bar is for the test column without external supplemental energy dissipation and the second is for the column with added mild steel yielding devices. From Figure 3(a), it can be seen that the one plastic hinge model slightly over predicts column lateral displacement for the column without supplemental damping, while it slightly under estimates lateral displacement in the moderate drift range for columns with the external energy dissipation devices. However, it is also seen in Figure 3 (b) that the two hinge model also over estimates column displacement, particularly so for moderate to high drift levels. Based on this, it seems that the one plastic hinge model provides adequate prediction of column lateral displacement response. Moreover, the rotation observed at the top of the first segment in the column with supplemental energy dissipation devices is a direct result of the fact that they strengthened (and stiffened) the column base but not other sections above it. It is expected that other energy dissipation options such as longitudinal mild steel yielding rebar will be included along the full column height, and the local stiffening observed in this work will be avoided, thereby concentrating column rotation at the base of the column.

One additional key result of the experimental work by Chou and Chen is the determination of plastic hinge length from the data. The work by Hewes and Priestley assumed a plastic hinge length of  $L_p = 0.5D$ , where  $D$  is the outside diameter of the column. These researchers found the plastic hinge length to be approximately  $0.58D$ , which correlates well with the one-half section diameter value.

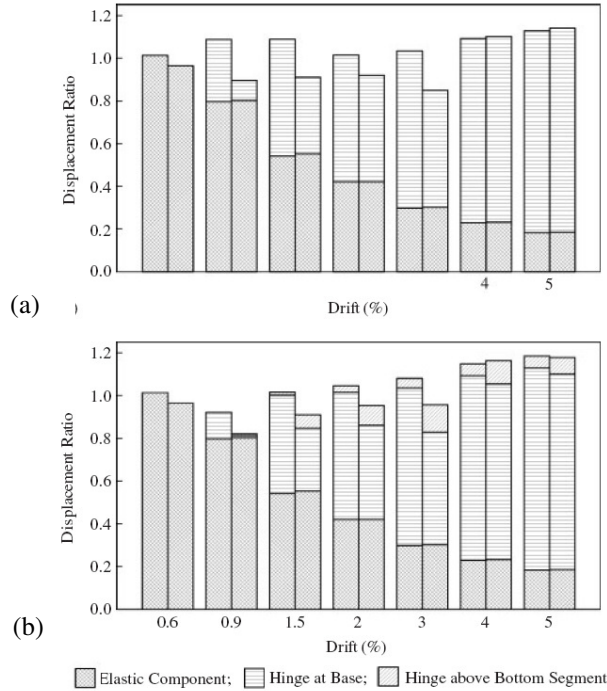


**Fig. 3 Distribution of lateral displacement component (a) one plastic hinge model (b) two plastic hinge model (from Chou and Chen)**

CORNELL UNIVERSITY

Researchers at Cornell University examined the performance of precast segmental unbonded post-tensioned columns which included engineered cementitious composites or “ECC”, also called ductile fiber-reinforced cement-based composites or “DFRCC”, in the base segments near the region of maximum moment demand. The research reported on by Billington and Yoon<sup>10</sup> consisted of experimental testing of seven different unbonded PT columns, four characterized as “short” and three as “tall”. The primary aspects investigated in the work was the influence of the DFRCC on column damage near the base where flexural demands and rotations are highest, and on overall column energy dissipation. Use of the DFRCC was hypothesized to eliminate the need for mild steel rebar for supplemental damping purposes, which would lead to reduced construction time and costs of the unbonded PT column system. Small – scale square columns with 200 mm width were utilized along with four post-tensioned 9.5 mm seven-wire strands which were each located near a corner of the section. For each column height, one test specimen used a conventional concrete mix design for the entire column, thus providing a benchmark for comparison of the influence of the DFRCC materials. Additionally, the researchers investigated the influence of socket depth of the base segment into the footing, with one column in each height group having a 76 mm socketed depth while all others had a column base 38 mm below the surface of the foundation.

Results of the research indicated that the DFRCC enhanced the energy dissipation of the unbonded PT short columns up to moderate drift levels, but had less influence at drift levels greater than about 3%. For the tall height columns, the DFRCC had relatively less significant

effects on total energy dissipation, but the enhanced energy absorption was more constant across drift level. The researchers observed that once a large flexural crack opened at the base of the column, the deformation of DFRCC within the base segment decreased thus reducing the energy dissipation within the DFRCC. The explanation for the more significant increase of energy dissipation for the short columns is that a relatively taller portion of the short columns contained DFRCC – the base segment heights for short columns were identical to those in the corresponding tall columns thus leading to the higher proportion of DFRCC in the short columns. The researchers found also that the tall height column with 76 mm base socket depth dissipated more energy than that with a 38 mm embedment. They attributed this to the fact that with a taller segment height the segment's (non-continuous) longitudinal mild steel was able to be more fully developed thereby allowing for more regions of the steel to yield.

As a general rule, for drifts of about 1% and greater, the experimental results indicate that the DFRCC increased energy absorption by approximately 50% as compared to columns utilizing conventional concrete throughout the column height. Since unbonded columns without any supplemental damping typically exhibit equivalent viscous damping ratios on the order of 5% to 8%, it would appear that use of DFRCC can be expected to increase equivalent viscous damping to approximately 8% to 12%. These levels of damping may not be sufficient to control maximum seismic displacement demands and are significantly less than those achieved in the hybrid columns with dissipative mild steel described previously (see Figure 2). Other observations from the research program included the negligible residual drift of all of the test columns, even after excursions to 10% lateral column drift. Maximum residual drifts on the order of 0.2% were reported, and no spalling of concrete materials was noted in the columns with DFRCC. This result may provide support for utilization of DFRCC in the base regions of unbonded PT columns as it appears that it can almost entirely eliminate earthquake damage that requires costly repairs.

#### SUNY – BUFFALO & NATIONAL TAIWAN UNIVERSITY

A collaborative, comprehensive analytical and experimental research program focused on the analysis, design, and performance of precast segmental bridge columns with unbonded tendons was conducted by researchers at the State University of New York – Buffalo and the National Taiwan University (Ou, Wang, Tsai, Chang, and Lee<sup>11</sup>). Large scale columns with unbonded tendons and additional longitudinal mild steel rebar for energy dissipation (“ED”) were constructed and tested under simulated lateral earthquake loading, and a total of four test specimens were constructed. The stated objectives of the research were: 1. “...to verify the proposed construction method and seismic detailing for the mild steel bars that are continuous across the segment joints”, and 2. “...to investigate the seismic behavior of the proposed columns with different ED bar ratios and posttensioning forces.”

Each column consisted of a precast footing, four precast column segments with square hollow sections, and a precast capbeam. Overall specimen height was 5.70 m from base of footing to top of capbeam, and the column segment section was 0.86 m in width/height. Of the four specimens, one contained only unbonded tendons across the segments (“C0C”), two

included energy dissipation longitudinal mild steel rebar in the amount of 0.5% (“C5C” & “C5C-1”), and one included 1% energy dissipation longitudinal rebar (“C8C”). The longitudinal energy dissipation steel ran the full height of the columns from the footing to capbeam, and was unbonded over a small length at the column base at the footing level. Specimens C0C, C5C, and C8C contained four unbonded tendons located in the hollow portion of the column section (interior cell) with a post-tensioning force corresponding to  $0.07f'_cA_g$ , while specimen C5C-1 contained significantly less post-tensioning equal to  $0.02f'_cA_g$ . An externally applied axial gravity load corresponding to  $0.10f'_cA_g$  was also applied to each test column. Column segments contained cross ties for confinement. All columns were tested as cantilevers with lateral point loading applied at the capbeam level.

This research work is significant because it: demonstrated a straight-forward process for assembling precast columns that include additional mild steel for enhanced energy dissipation characteristics, detailed a method for calculating the required unbonded ED bar length to avoid premature fracture of the bars due to low cycle fatigue, illustrated the re-centering tendency of the columns even with yielding mild steel (ED bars), and similar to other experimental research programs illustrated the improved resistance to seismic induced damage as compared to conventional monolithic RC construction. All test units exhibited stable, ductile force – displacement hysteretic response up to the maximum imposed column drift of 5%. Spalling of cover concrete was first observed at 4% drift, and was of an extent that could be easily repaired. ED bars remained intact (no fracture or buckling) up to 5% drift, and as the amount of ED reinforcement was increased, the columns exhibited increased energy dissipation as evidenced by fattened hysteresis loops. For units with 0.5% ED steel, residual drift at the end of testing after all lateral loads were removed was small and on the order of 0.5%. A conventional RC column designed to achieve the same peak drift would have on the order of 2% post-earthquake residual drift and would require complete replacement. The equivalent viscous damping of the test units with 0.5% ED steel calculated at the maximum imposed drift was 16% to 18%, which is only very slightly smaller than what would be expected in a conventional RC column designed to the same drift level. Thus, maximum displacements of hybrid columns can be expected to be very similar to those for conventional RC columns.

#### WASHINGTON STATE UNIVERSITY

Whereas all research described previously above focused on the analysis and design of individual unbonded post-tensioned columns, work at Washington State University (ElGawady and Sha'lan<sup>12</sup>) investigated the behavior of re-centering two column bridge bents. Five, one-quarter scale bents were constructed and tested under simulated lateral seismic loading. One subassemblage unit was constructed using conventional cast-in-place RC construction for both the columns and the cap beam, and this specimen served as a benchmark for comparing the performance of the re-centering units. The other four test units utilized precast column segments reinforced longitudinally with unbonded post-tensioning and a conventionally reinforced RC cap beam. The precast segments used fiberglass composite tubes to serve as both the formwork and transverse reinforcement, and did not contain any longitudinal rebar in addition to the single unbonded tendon located at the center

of the circular column section. Of the four re-centering bents, one contained columns that were precast as a single full column height segment (“FRP-1”), and the other three used columns which were constructed from three equal height precast segments (“FRP-3”, “FRP-3-S”, “FRP-3-R”). Of the three units with stacked segments, one used a neoprene rubber pad at the interface between the top of the column and cap beam soffit (FRP-3-R), and another incorporated ASTM A36 steel angles at the column-foundation and column-cap connection joints in order to enhance energy dissipation of the system (FRP-3-S). The re-centering bents utilized a post-tensioning force that produced an initial axial force ratio, AFR, of approximately 0.30. This level of initial post-tensioning was selected so that FRP-1 and FRP-3 would achieve approximately the same lateral strength as the benchmark RC unit at the design drift level.

Experimental test results demonstrated that bridge bents can be designed to experience less residual deformation after a significant seismic event through the use of re-centering columns with unbonded post-tensioning. In general, the re-centering bents exhibited less total damage than the benchmark conventional RC specimen. After yielding, the RC column bent exhibited residual drifts on the order of 50% of the peak imposed lateral drift, while the re-centering bents experienced residual drifts of about 5% to 10% of the peak imposed drifts. At 6.9% lateral drift, columns in the conventional RC bent experienced significant cover concrete spalling and longitudinal rebar buckling, and the lateral strength dropped by 20%. For all of the re-centering bents, lateral strength was maintained up to the peak imposed drift of approximately 9% (except for one direction of loading in unit FRP-3-S where the anchors for the mild steel angles pulled out due to inadequate anchorage). For the practical range of design drift – say 5% or less – the re-centering bridge bents demonstrated superior performance with respect to damage level. However, energy dissipation in all of the re-centering bents was very low compared to that in a traditional RC column. This is evidenced by the thin, pinched hysteretic loops in the lateral force – displacement response of the re-centering units. For example, at a drift of 4%, the RC equivalent viscous damping was approximately 14%, while the average for the re-centering units was about 4.5%. FRP-3-S with the added mild steel angle for energy dissipation did not achieve damping levels much higher than the units without supplemental energy dissipation, and at 4% drift its equivalent viscous damping was about 6.5%.

In summary, the research by ElGawady and Sha’lan served as a “proof-of-concept” whereby the unbonded post-tensioned column was incorporated into a bridge bent subassemblage, and through physical testing it was shown to possess improved damage tolerance attributes when compared to response of traditional cast-in-place reinforced concrete construction. The research also demonstrated that fiber composite tubes can provide an efficient means of forming precast segments, as well as provide structural transverse reinforcement. Limitations to the work include the relatively small scale – columns used were 204 mm in diameter – and the poorly anchored yielding mild steel angles which prevented the specimen from achieving higher levels of supplemental damping.

## CRITICAL DESIGN ISSUES

### AXIAL FORCE RATIO

Few researchers have addressed specifically what level of column initial axial stress is considered “ideal” in the design of re-centering columns. Because this parameter influences the ductility of the unbonded PT column (with or without supplemental damping), it is critical that an acceptable range of axial force ratios be identified, with particular attention to the upper limit as undesirable response can result with too high of an initial column compression stress. Hewes and Priestley recommended an upper limit of about 0.2 to 0.25, and this certainly serves as an initial guide, but further research should study this issue. Figure 1 (b) above depicts in a general sense how AFR influences second-slope stiffness, but studies investigating under what set of conditions does the force – displacement stiffness become negative should be undertaken. For now, engineers could use the simple analytical models to predict the full force – displacement response of a given column design in order to evaluate whether the design provides ductile, stable behavior.

Also related to column axial compression stress is the tendon stress level after post-tensioning and after time dependent losses have occurred. To maximize efficiency in the use of post-tensioning, one would select a high initial prestress level. However, the tendon initial stress should be chosen such that the stretching or lengthening of the tendon under lateral loading to the design displacement does not induce yielding of the tendon, which would lead to partial loss of column post-tensioning force and the re-centering benefit it provides. Tendon lengthening can be related to column drift,  $\theta$ , location of tendon within the section,  $d_i$ , tendon unbonded length,  $L_o$ , and neutral axis depth,  $c$ . Figure 4 below shows a close-up view of the base segment of a column with an idealized rigid rotation about the column compression toe. With the geometry shown, the tendon incremental tensile strain,  $\Delta\epsilon_{ps}$ , can be calculated as:

$$\Delta\epsilon_{ps} = \theta \frac{(d_i - c)}{L_o} \quad (3)$$

Thus, knowing the column drift and neutral axis position for that drift, one can determine the increase in tendon strain due to gap opening at the column base. Rather than require the engineer to use the analytical model to iterate for neutral axis depth for the particular column design and drift level, it would be useful if researchers developed expressions that could easily be incorporated into design codes for incremental tendon strain,  $\Delta\epsilon_{ps}$ , as a function of the column initial AFR, drift, column section depth, and location of tendon within the section. This approach has been in fact implemented for similar types of structural elements such as post-tensioned masonry walls with unbonded tendons.

Another feasible approach to facilitating the determination of tendon stress at a particular drift level would be to develop a series of tables with tendon incremental stress increase,  $\Delta f_{ps}$ ,

as a function of various design parameters including the AFR, column aspect ratio,  $L/D$ , column drift,  $\theta$ , and concrete compression strength,  $f'_c$ . An example of such a table is shown in Tables 1 and 2 below, which are taken from Hewes<sup>3</sup>. Table 1 provides values of incremental tendon stress increase at 3% overall column drift for an AFR of 0.20, while Table 2 shows the same for an AFR of 0.25. The 2%, 3%, and 4% headings in the tables refer to the level of transverse confinement provided at the column base, which influences to some degree the neutral axis depth for a given total axial column force. The data shown in the tables could also be provided graphically and used a “tool” in the design process of unbonded PT columns, and an example of such a graph is shown in Figure 5. The graph shows different curves for tendon stress increase for varying levels of lateral confining stress,  $f_l$ , provided by transverse reinforcement. As is evident, this variable does not have great influence on stress increase,  $\Delta f_{ps}$ , and for design purposes the curves could be combined into an average that is representative of the common ranges of transverse confinement level.

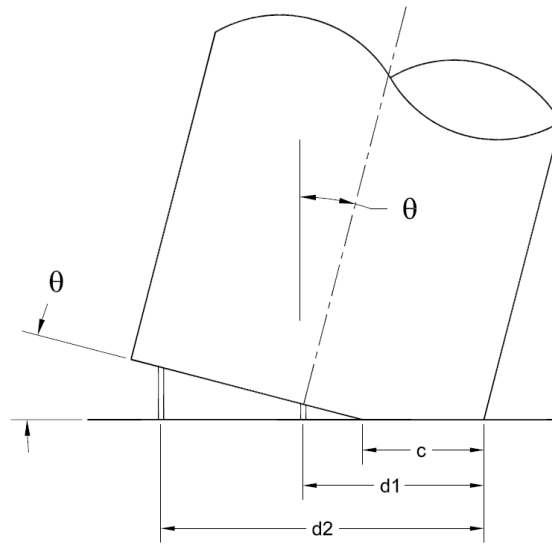


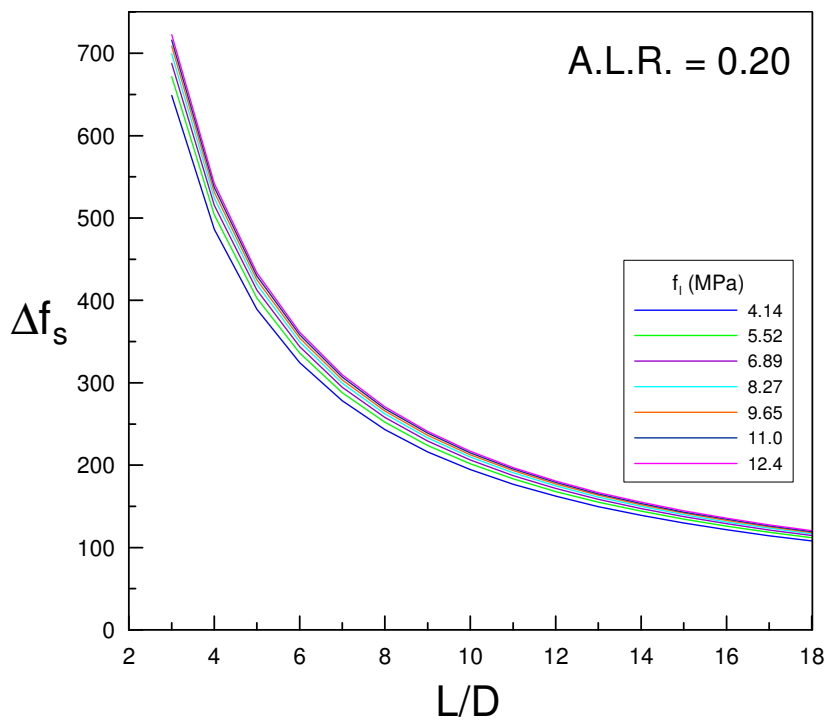
Fig. 4 Close-up view of gap opening at base of column with unbonded post-tensioning

Table 1  $\Delta f_{ps}$  for 3.0% drift and ALR=0.20, and  $f'_c = 55$  MPa

L/D	2%	3%	4%
3	75.7	80.0	82.5
4	56.4	60.0	61.9
5	45.4	48.0	49.5
6	37.8	40.0	41.3
7	32.4	34.3	35.4
8	28.3	30.0	30.9
9	25.2	26.6	27.5
10	22.7	24.0	24.7
11	20.6	21.8	22.5
12	18.9	20.0	20.6

**Table 2  $\Delta f_{ps}$  for 3.0% drift and ALR=0.25, and  $f'_c = 55$  MPa**

L/D	2%	3%	4%
3	64.0	70.2	73.5
4	48.0	52.6	55.1
5	38.5	42.1	44.1
6	32.0	35.1	36.7
7	27.4	30.0	31.5
8	24.0	26.3	27.5
9	21.3	23.4	24.5
10	19.2	21.0	22.0
11	17.5	19.1	20.0
12	16.0	17.5	18.3



**Fig. 5 Tendon incremental stress increase versus column aspect ratio (from Hewes<sup>3</sup>)**

**DESIGN METHOD**

Traditionally, structural engineers have designed structures for earthquake loading using what has been called “force based design”, which simply means that lateral seismic forces are the key “driver” in the design process. Acknowledging that it is not economically practical to design structures to remain in the elastic range under moderate to high earthquake loading, force based design uses a reduced lateral design force which leads to inelastic structural response and some level of “acceptable” structural damage. The key to force based design has been the development of general relations between the force reduction factor,  $R$ , and the inelastic deformation demands to be expected during the design level earthquake.

These relations that have been shown to be somewhat reliable are based on well-established assumed hysteretic response rules, which are not representative of the flag-shaped re-centering hysteretic behavior of columns with unbonded tendons. Specifically, the hysteretic rules used to develop current  $R-\mu$  relationships contain significant hysteretic energy dissipation which models accurately the observed response of structural elements such as conventionally reinforced concrete beams and columns and yielding steel structural elements. Figure 6 below illustrates the marked difference in expected energy dissipation as represented by the area contained within the hysteretic loops, where Figure 6 (c) shows that an unbonded PT column will possess little ability to dissipate seismic input energy. Thus, if force based design is to be used to design re-centering columns, researchers will need to study how inelastic displacement demands are influenced by parameters such as amount of supplemental damping and tendon post-tensioning force, and will need to develop new  $R-\mu$  relationships appropriate for re-centering columns.

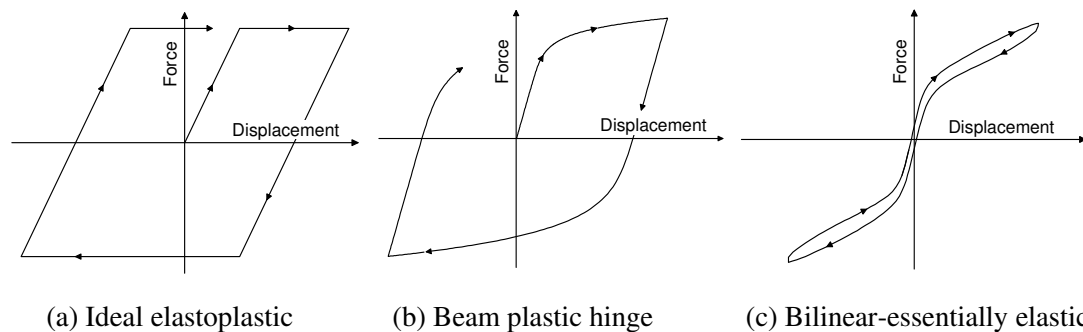


**Fig. 6 Various hysteretic behaviors (from Hewes<sup>3</sup>)**

An alternative to force based design is the direct displacement-based design (DDBD) method first proposed by Priestley<sup>13</sup>. In that procedure, structural displacement is the “driver” instead of seismic force since damage and performance are better correlated to structural deformations than force. The procedure, which is not described in detail here, requires an estimation of structural damping at the given design displacement, and thus relationships and/or design equations for damping versus ductility similar to those shown in Figure 2 (b) need to be refined and adopted. Standardized curves for damping versus ductility need to be developed that cover the range of re-centering ratios  $\lambda$  that are expected to be used in design. The approach of New Zealand design code NZS 3101:2006 which weights equivalent damping according to the relative contributions of re-centering and mild steel dissipative moments to the total moments would appear to be overly conservative as evidenced by the significant under estimation of equivalent viscous damping when compared to actual experimental test results (see Figure 2). It seems researchers could develop a new expression or series of expressions for damping versus ductility using the two rotational spring modeling approach described in Palermo et al<sup>5</sup>.

An outline of the steps for a proposed design procedure utilizing DDBD is given as:

1. Select design parameters

$$H = \text{column height [meter]}$$

$M$  = lumped seismic mass at column top [kg]

$\theta_D$  = design drift [radian]

$f'_c$  = concrete compressive strength [MPa]

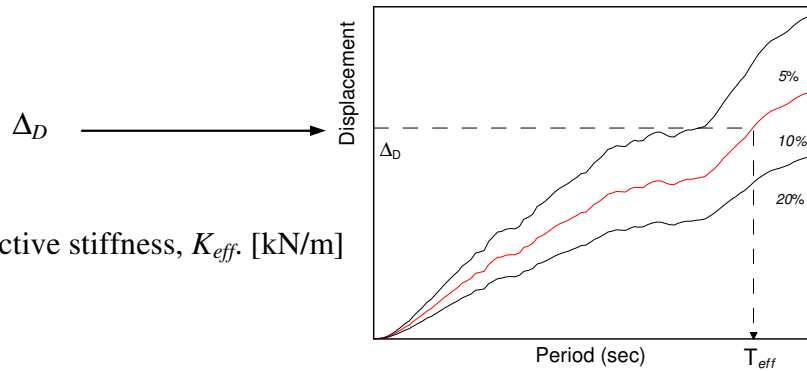
$\epsilon_s$  = prestressing steel limit strain at design drift [m/m]

$\lambda$  = re-centering ratio (which can be related to amount of supplemental yielding mild steel)

2. Calculate displacement ductility demand,  $\mu_D$ , from yield displacement,  $\Delta_y$ , and design displacement,  $\Delta_d$ . As a first iteration in the design process, the yield drift can be estimated as 0.5%.

3. Using the estimated displacement ductility demand, and either expressions or graphs of equivalent viscous damping versus ductility (such as those in Figure 2 (b)), determine the column damping,  $\xi_{Equiv Visc}$  [%].

4. Using elastic displacement response spectra for the design seismic event, determine the column effective period by entering the spectra graph along the vertical axis with design displacement, reading horizontally across to the intersection of the appropriate damping curve, and then down vertically to the intersection of the structural period,  $T_{eff}$  [seconds].



5. Calculate effective stiffness,  $K_{eff}$  [kN/m]

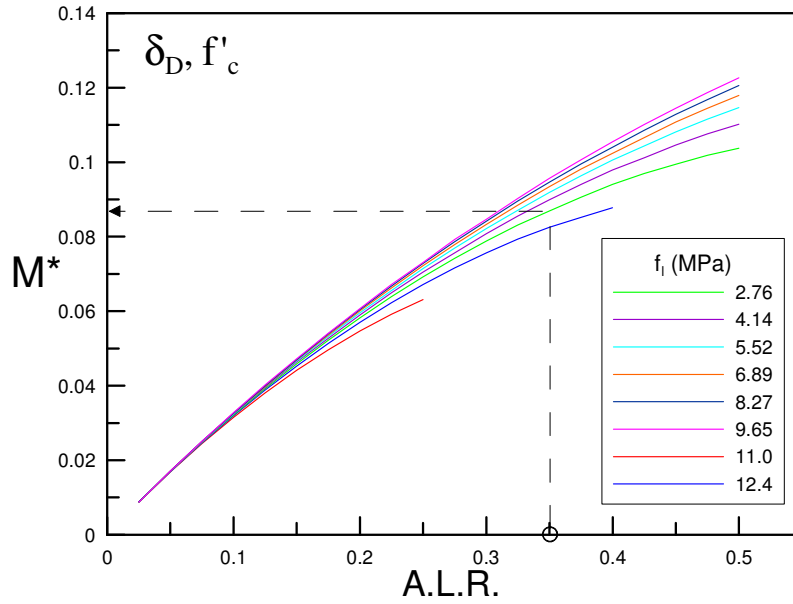
$$K_{eff} = \frac{4\pi^2 M}{T_{eff}^2} \tag{4}$$

6. Calculate design lateral force,  $F_D$  [kN], and moment,  $M_D$  [kN-m]

$$F_D = K_{eff} \times \Delta_D \tag{5}$$

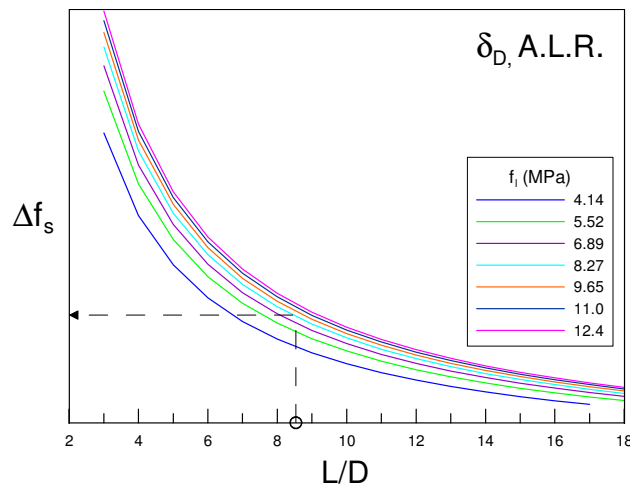
$$M_D = F_D \times H \tag{6}$$

7. Determine column diameter. Choose AFR and column base lateral confinement stress,  $f_i$ , and read off dimensionless moment,  $M^*$ , from graph:



$$M^* = \frac{M_D}{f'_c D^3}, \quad \therefore D = \sqrt[3]{\frac{M_D}{f'_c M^*}} \tag{7}$$

8. Determine  $\Delta f_{ps}$  [MPa],  $f_{si}$  [MPa], and  $A_s$  [mm<sup>2</sup>]. Go to chart for  $\theta_D$  and chosen AFR to determine  $\Delta f_{ps}$ , from known L/D and confinement level chosen above.



$$f_{psi} = f_{ps} - \Delta f_{ps} = \epsilon_{ps} E_{ps} - \Delta f_{ps} \quad (8)$$

The prestressing steel area  $A_s$  is determined using the design limit steel strain,  $\epsilon_s$ , and the definition of the design axial force ratio,  $AFR$ .

$$AFR = \left[ \frac{N + F_{ps} + \Delta F_{ps}}{f'_c A_c} \right] \quad (9)$$

$$(F_{psi} + \Delta F_{ps}) = A_s f_{ps} = A_s \epsilon_{ps} E_{ps} \quad (10)$$

$$A_s = \left[ AFR \times f'_c A_c - N \right] \frac{1}{\epsilon_{ps} E_{ps}} \quad (11)$$

The non-dimensional moment capacity charts such as that shown above can be created using the simple analytical model utilized by Pampanin<sup>7</sup> which accounts for the presence of energy dissipation mild steel rebar at the column base connection. These charts can be created for typical locations of tendons and energy dissipation steel, which can be expressed as a fraction of the column section depth in a fashion similar to what has been done for conventional reinforced concrete column design charts.

## SUMMARY

The significant research efforts reviewed in this paper have contributed to the body of knowledge on the analysis and design of re-centering bridge columns, and this technology is essentially ready to be applied to real bridge projects where rapid construction and reduced overall seismic damage are desired. A sufficient number of physical destructive tests on large scale test units have been performed so that bridge owners can feel confident in the stability and ductility of re-centering columns under high seismic loading such as is found in parts of California and Washington. What is needed at this juncture is an assembling of all of the research findings into logical, safe design specification that would aid practicing engineers in the design of this new structure type. These design specifications should address: design method and steps, guidance on level of initial axial force (post-tensioning and gravity load), simple expressions to relate amount of energy dissipation steel (yielding mild steel) to damping level as a function of lateral drift, confinement requirements at critical column sections (maximum moment sections where significant gap opening is expected), and an analytical method to predict the force – displacement response of columns. One area that is

still not yet fully developed is the establishment of performance limits with quantifiable expected damage levels.

## REFERENCES

1. Hewes, J., and Priestley, M.J.N., "Seismic Design and Performance of Precast Concrete Segmental Bridge Columns," Structural Systems Research Project, Report No. SSRP – 2001/25, University of California, San Diego, La Jolla, California. May 2002.
2. Hewes, J., "Seismic Tests on Precast Segmental Concrete Columns with Unbonded Tendons," *Bridge Structures*, V. 3, No. 3-4, December 2007, pp. 215-227.
3. Hewes, J., Seismic Design and Performance of Precast Concrete Segmental Bridge Columns, Ph.D. Dissertation, University of California, San Diego, La Jolla, California. December 2002.
4. Marriott, D., Boys, A., and Pampanin, S., "Experimental Validation of High-Performance Hybrid Bridge Piers," *Proceedings of the New Zealand Society for Earthquake Engineering Conference*, March 2006, Napier, New Zealand, Paper No. 19.
5. Palermo, A., Pampanin, S., and Marriott, D., "Design, Modeling, and Experimental Response of Seismic Resistant Bridge Piers with Posttensioned Dissipating Connections," *Journal of Structural Engineering*, V. 133, No. 11, November 2007, pp. 1648-1661.
6. Marriott, D., Pampanin, S., and Palermo, A., "Quasi-static and Psuedo-dynamic Testing of Unbonded Post-Tensioned Rocking Bridge Piers with External Replaceable Dissipaters," *Earthquake Engineering and Structural Dynamics*, V. 38, No. 3, March 2009, pp. 331-354.
7. Pampanin, S., Priestley, M.J.N., and Sritharan, S., "Analytical Modeling of the Seismic Behavior of Precast Concrete Frames Designed with Ductile Connections," *Journal of Earthquake Engineering*, V. 5, No. 3, 2001, pp. 329-367.
8. Chou, C-C., and Chen, Y-C., "Cyclic Test of Post-Tensioned Precast CFT Segmental Bridge Columns with Unbonded Strands," *Earthquake Engineering and Structural Dynamics*, V. 34, No. 2, February 2006, pp. 159-175.
9. Chou, C-C., and Hsu, C-P., "Hysteretic Model Development and Seismic Response of Unbonded Post-tensioned Precast CFT Segmental Bridge Columns," *Earthquake Engineering and Structural Dynamics*, V. 37, No. 6, May 2008, pp. 919-934.
10. Billington, S., and Yoon, J., "Cyclic Response of Unbonded Posttensioned Precast Columns with Ductile Fiber-Reinforced Concrete," *ASCE Journal of Bridge Engineering*, V. 9, No. 4, July-August 2004, pp.353-363.
11. Ou, Y-C., Wang, P-H., Tsai, M-S., Chang, K-C., and Lee, G., "Large-Scale Experimental Study of Precast Segmental Unbonded Posttensioned Concrete Bridge Columns for Seismic Regions," *ASCE Journal of Structural Engineering*, V. 136, No. 3, March 2010, pp. 255-264.
12. ElGawady, M., and Sha'lan, A., "Seismic Behavior of Self-Centering Precast Segmental Bridge Bents," *ASCE Journal of Bridge Engineering*, V.16, No. 3, May 2011, pp. 328-339.
13. Priestley, M.J.N., "Direct Displacement-Based Design of Precast/Prestressed Concrete Buildings," *PCI*, V. 47, No. 6, pp. 66-78.